Desalination and Water Treatment
www.deswater.com
doi: 10.1080/19443994.2014.950344

56 (2015) 1389–1402
October

Taylor & Francis
Taylor & Francis Group

Response surface methodological evaluation of the adsorption of textile dye onto biosilica/alginate nanobiocomposite: thermodynamic, kinetic, and isotherm studies

R. Darvishi Cheshmeh Soltani[a,*], A.R. Khataee[b], H. Godini[c], M. Safari[d], M.J. Ghanadzadeh[a], M.S. Rajaei[a]

[a]*Department of Environmental Health Engineering, School of Health, Arak University of Medical Sciences, Arak, Iran, Tel. +98 86 33662024; Fax: +98 86 33686443; emails: darvishi@arakmu.ac.ir (R. Darvishi Cheshmeh Soltani), mjghanad@arakmu.ac.ir (M.J. Ghanadzadeh), msrajaei@yahoo.com (M.S. Rajaei)*
[b]*Faculty of Chemistry, Research Laboratory of Advanced Water and Wastewater Treatment Processes, Department of Applied Chemistry, University of Tabriz, Tabriz, Iran, Tel. +98 411 3393165; Fax: +98 411 3340191; email: a_khataee@tabrizu.ac.ir (A.R. Khataee)*
[c]*Faculty of Health, Department of Environmental Health Engineering, Lorestan University of Medical Sciences, Khorramabad, Iran, Tel. +98 9163611395; email: h_godini@yahoo.com (H. Godini)*
[d]*Department of Environmental Health Engineering, School of Health, Kurdistan University of Medical Sciences, Sanandaj, Iran, Tel. +989188128262; email: safari.m.eng@gmail.com (M. Safari)*

Received 23 April 2014; Accepted 7 July 2014

ABSTRACT

The present investigation was carried out to synthesize biosilica/calcium alginate (CA) nanobiocomposite and evaluate the efficiency of as-prepared adsorbent for removing Direct Blue 71 (DB71) from aqueous solutions. Response surface methodology based on central composite design was applied to optimize the process. Accordingly, the maximum color removal of 81.49% was achieved at an initial DB71 concentration of 21 mg/L, adsorbent dosage of 2.4 g/L, contact time of 42 min and initial pH of 5. The negative values of Gibbs free energy (ΔG°) and enthalpy change (ΔH°), which were obtained during the thermodynamic study, revealed spontaneous and exothermic nature of the adsorption process, respectively. The adsorption of DB71 onto the nanobiocomposite followed pseudo-second-order kinetic model (R^2 = 0.977) and Langmuir isotherm model (R^2 = 0.994). The maximum adsorption capacity of biosilica/CA nanobiocomposite for the adsorption of DB71 was found to be 21.32 mg/g. The value of mean free energy (12.91 kJ/mol) indicated chemical adsorption of DB71 onto the adsorbent.

Keywords: Nano-siliceous adsorbent; Nanocomposite; Biocomposite; Adsorption; Experimental design

1. Introduction

Discharging colored effluents into aqueous environments such as rivers and lakes can cause detrimental effects on aquatic life [1,2]. Among various chromogenic substances, azo dyes are the largest category discharged by various industries such as textile, food, paper, cosmetic, leather, and plastic [3,4]. Since azo dyes or their metabolites are toxic and potentially carcinogenic, the presence of organic azo

*Corresponding author.

dyes can cause threat to human health [3]. Therefore, the purification of colored effluents by several physical and chemical technologies has been considered [5–7]. Among different physicochemical technologies, the application of adsorption process has gained much more attention due to its simplicity, cost-efficiency, ease of operation, and low sensitivity to toxic environments [4–6,8–10]. In recent years, many researchers have focused on the use of locally available adsorbents such as clay minerals [11], agricultural wastes [12,13], and natural polymers [14] for removing organic dyes from aqueous solutions instead of expensive activated carbon. It has been reported that the silica-based materials can be used as efficient adsorbents due to the capability of their functional groups for sequestering target pollutants [15–17]. Thus, in the present study, the application of a siliceous adsorbent named biosilica was considered for treating colored solutions. Biosilica is a biological sedimentary rock composed of nearly 90% silica, which is suitable for the adsorption of organic dyes because of its high surface area containing surficial functional groups [4]. However, it is difficult to withdraw and recover fine biosilica particles after the adsorption for subsequent utilization. Therefore, the immobilization of biosilica within a suitable material was taken into account to avoid releasing the particles into the environments and make the process cost-efficient. In addition, the immobilization of fine adsorbents is an essential step for full-scale applications [4,8,18]. Many polymeric substances such as alginate [8,19,20], chitosan [18,20], polyethyleneimine [21], carboxy methyl cellulose [20], and polyvinyl alcohol [20,22] have been applied for the entrapment of different fine adsorbents. Alginate, as a natural carbohydrate polymer derived from brown algae, has been widely employed for the immobilization of various adsorbents because of its biodegradability, hydrophilicity, mechanical stability, and ease of preparation [3,8]. Moreover, high potential of the alginate matrix for the adsorption of organic dyes has been demonstrated [19,23]. Therefore, the utilization of alginate can be an efficient alternative for the immobilization of fine adsorbents such as biosilica. Hence, in the present study, biosilica particles were incorporated into the alginate matrix and used as adsorbent for the removal of an azo dye (Direct Blue 71 (DB71)) from aqueous solutions. The toxicity of direct dyes to living organisms such as *Daphnia magna* has been demonstrated [24,25]. To the best of our knowledge, there is no report on the use of immobilized biosilica within calcium alginate (CA) for the adsorption of organic dyes in aqueous phase. To evaluate the effect of various operational parameters, response surface methodology (RSM) based on central composite design (CCD) was applied as statistical approach. Reduced number of experimental runs, capability to evaluate the interactive effects of the operational parameters, and possibility to optimize the operational parameters for achieving maximum efficiency are the advantages of RSM approach in comparison with the conventional one-factor-at-a-time statistical strategy [26–30]. In the next step, thermodynamic, kinetic, and isotherm studies were carried out to reach a better understanding of the adsorption process designed for the removal of DB71.

2. Materials and methods

2.1. Chemicals

Direct blue 71 (an anionic azo dye with molecular formula: $C_{40}H_{23}N_7Na_4O_{13}S_4$ and molecular weight: 1029.87 g/mol) was purchased from Nasaj Sabet Company, Iran, and used without any purification. Nano-sized biosilica (molecular weight of 1.495 g/mol, and SiO_2 basis >95%), which was of analytical grade, was purchased from Sigma-Aldrich, USA. Sodium alginate from *Laminaria hyperborean* was purchased from BDH Laboratory Supplies (Poole, England) and used for the immobilization of biosilica particles. All other reagents and chemicals were of analytical grade and were obtained from Merck, Germany. The pH of solutions was adjusted using 0.1 M NaOH or 0.1 M HCl.

2.2. Preparation of biosilica/CA nanobiocomposite

To immobilize the adsorbent, 20 g of nano-sized biosilica was mixed in 500 mL of 2% sodium alginate solution. The mixture was magnetically stirred for 1 h at 100 rpm to reach a homogeneous mixture and was kept for a day to obtain a bubble-free blend. The resulted compound was added dropwise via a syringe to 1 L of 0.5 M calcium chloride solution. Calcium atoms can create salt bridges between the α-L-guluronic acids (G) blocks of alginate matrix to form CA. As a result of above-mentioned reactions, the immobilized adsorbent was in bead form. After keeping the beads in calcium chloride for 24 h, the beads were withdrawn from the solution and washed with deionized water to remove impurities. Then, they were dried at room temperature until achieving actual size [8]. Finally, the beads were ground and sieved using standard sieves. The size distribution of applied beads was between 10 and 20 mesh.

2.3. Experimental proceedings and design

Batch experimental runs were carried out using 100-mL Erlenmeyer flasks. These flasks were placed

on a shaker and thoroughly stirred. Additionally, a shaker incubator (Model: ISH 554D, Fannavarane Sahand Azar, Iran) was applied for conducting thermodynamic study. CCD model was used to evaluate the effect of four main operational parameters influencing the adsorption of DB71 onto biosilica/CA nanobiocomposite, including initial DB71 concentration (mg/L), adsorbent dosage (g/L), contact time (min), and initial pH. The number of experimental runs was calculated via Eq. (1):

$$N = 2^k + 2k + x_0 \quad (1)$$

where N, k, and x_0 are the number of experiments, the number of operational parameters, and the number of replications as central points, respectively [31]. According to the aforementioned equation, the total number of experimental runs was obtained to be 31 (k = 4, x_0 = 7). An empirical second-order polynomial equation was employed to describe the relationship between the dependent parameter (color removal (%)) and the studied operational parameters as shown in Eq. (2):

$$Y = b_0 + \sum_{i=1}^{n} b_i x_i + \left(\sum_{i=1}^{n} b_{ii} x_i\right)^2 + \sum_{i=1}^{n-1} \sum_{j=i+1}^{n} b_{ij} x_i x_j \quad (2)$$

where Y is the predicted color removal (%) and b_0, b_i, b_{ij}, and b_{ii} are constant, linear, interaction, and quadratic coefficients, respectively. In addition, x_i and x_j are the coded values for the experimental parameters [27,29,32,33]. The experimental ranges and levels of the operational parameters concerning color removal are tabulated in Table 1. The ranges and levels of the operational parameters were selected based on the results of preliminary experiments.

2.4. Analytical procedure

Morphological structure of the biosilica/CA nanobiocomposite was analyzed via scanning electron microscopy (SEM) by means of a TESCAN microscope (Model: MIRA3, Czech Republic). In addition, Fourier transform infra-red (FT-IR) analysis was conducted using an infra-red spectrophotometer (Tensor 27, Bruker, Germany) in the wavenumber ranging from 400 to 4,000 cm^{-1} to assess the role of functional groups of the nanobiocomposite in the adsorption of DB71. For the measurement of residual DB71 concentration, the sample was taken out and centrifuged for 5 min at 5,000/min. Then, it was spectrophotometrically measured with a Hach UV–vis spectrophotometer (DR 5000, USA) at maximum wavelength of 577 nm.

3. Results and discussion

3.1. SEM and FT-IR analysis

To evaluate surface morphology of the biosilica/CA nanobiocomposite, SEM analysis was conducted and the results are depicted in Fig. 1. A rugged, uneven and porous surface for the nanobiocomposite can be observed in Fig. 1((a)–(d)), which is appropriate for the adsorption of target pollutant in aqueous phase. The results of our previous study indicated that biosilica is composed of nano-sized crystals (20 nm) and nano-porous structure with pore diameter size distribution ranging from 60 to 70 nm [4]. Furthermore, as can be obviously seen from Fig. 1((b)–(d)), the immobilization of nano-sized biosilica particles by CA has been performed appropriately. The presence of nano-sized biosilica adjacent to the CA is evidently shown in Fig. 1(b). As can be observed in Fig. 1(c), the immobilization of nano-sized biosilica within CA resulted in the formation of nanostructured beads on the surface of entrapped biosilica, which creates a suitable surface area for the adsorption process. In the following, FT-IR analysis was conducted to determine the role of various surficial functional groups on the adsorption of DB71. The presence of some main functional groups on the surface of biosilica/CA nanobiocomposite is evident in Fig. 2. As shown, the peaks centered at 3,400 cm^{-1} (corresponding to the stretching vibration of –OH, amino, and amide groups and their

Table 1
Ranges and levels of the experimental parameters for the adsorption of DB71 onto biosilica/CA nanobiocomposite

			Parameter level				
Run no.	Code	Parameter	−2 (α)	−1	0	+1	+2 (α)
1	X_1	Dye concentration (mg/L)	10	20	30	40	50
2	X_2	Adsorbent dosage (g/L)	0.5	1.0	1.5	2.0	2.5
3	X_3	Reaction time (min)	5	20	35	50	65
4	X_4	Initial pH	3	5	7	9	11

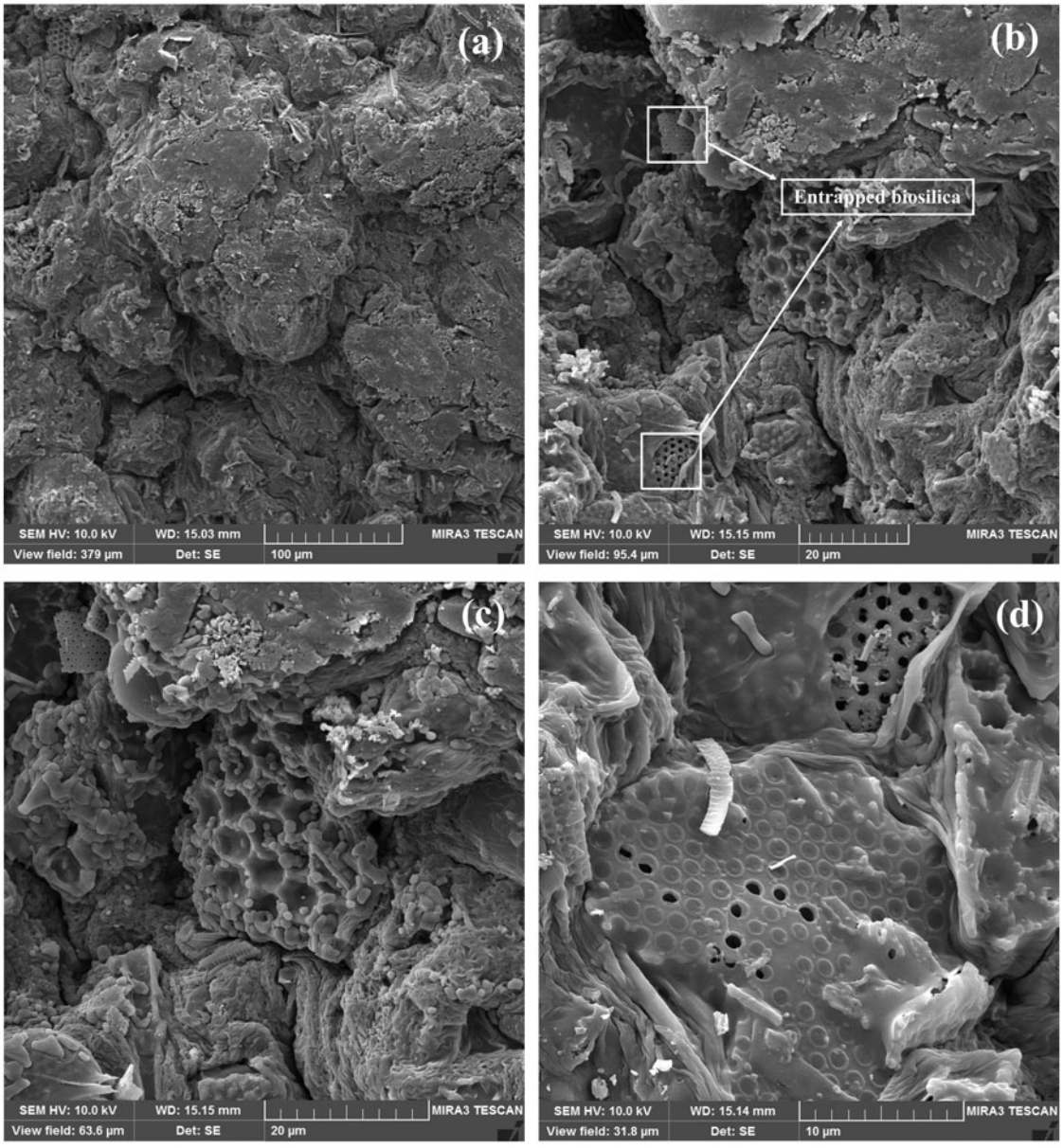

Fig. 1. SEM images of biosilica/CA nanobiocomposite at different magnifications ((a)–(d)).

overlapping) [14,23,34], 2,926 cm^{-1} (–CH band) [35], 1,641 cm^{-1} (–OH bending mode of adsorbed H_2O) [16], 1,762 cm^{-1} (stretching vibration of C=O from the carboxylic groups) [36], 1,454 cm^{-1} (–CH bending of alkene (in plane)) [4], 1,261 cm^{-1} (stretching vibrations of –CH bonds) [15], 1,050 cm^{-1} (Si–O–Si stretching) [37], 861 cm^{-1} (symmetric stretching of Si–O–Si) [38], 782 cm^{-1} (Si–O (out-of-plane) band) [39], and 480 (the Si–O–Si bond of condensed silica network) [16] were diminished after the adsorption of DB71, indicating that major portion of the functional groups placed on the surface of biosilica/CA nanobiocomposite are involved in the adsorption of DB71.

3.2. CCD results for decolorization of the dye

CCD model is one of the most widely applied statistical methods for the optimization of different operational parameters influencing the efficiency of experimental reactors [27,28,40–42]. Using CCD model, a second-order polynomial quadratic equation was obtained to describe mutual relationship between

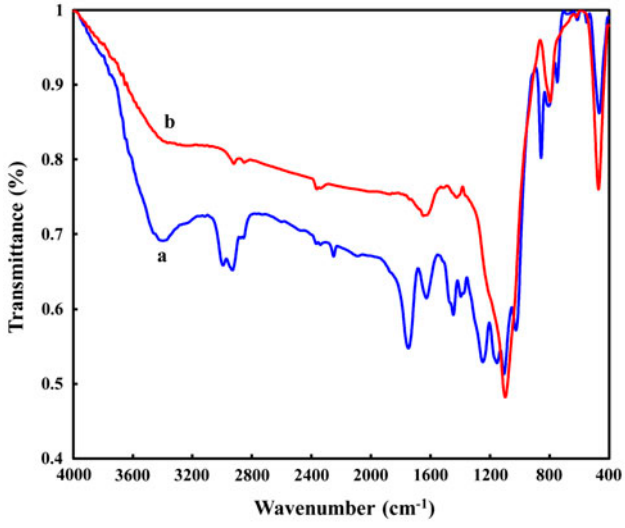

Fig. 2. FT-IR spectra of biosilica/CA nanobiocomposite before (a) and after (b) the adsorption of DB71.

different operational parameters (DB71 concentration (x_1), adsorbent dosage (x_2), contact time (x_3), and initial pH (x_4)) and specified response (color removal (%)), which is exhibited in Eq. (3):

$$Y(\mathrm{CR}(\%)) = 64.32 - 12.88x_1 + 6.21x_2 + 8.00x_3 - 3.94x_4 + 1.15x_1x_2 + 0.42x_1x_3 + 0.052x_1x_4 - 1.23x_2x_3 - 0.77x_2x_4 - 0.084x_3x_4 - 2.16x_1^2 - 2.68x_2^2 - 1.68x_3^2 - 1.61x_4^2 \quad (3)$$

The prediction of color removal (%) under different values of the operational parameters within the specified ranges can be achieved through Eq. (3). Based on Eq. (3), the experimental conditions (coded and actual parameters) together with experimental and predicted CR (%) are shown in Table 2. To assess significance of the CCD model for predicting the adsorption of DB71 onto biosilica/CA nanobiocomposite, analysis of variance (ANOVA) was performed [32,40,42]. The results of ANOVA are given in Table 3. The significance of the model can be checked by the correlation coefficients obtained via ANOVA [29]. The correlation coefficient was obtained using Eq. (4):

$$R^2 = 1 - (SS_{\mathrm{residual}}/SS_{\mathrm{model}} - SS_{\mathrm{residual}}) \quad (4)$$

where SS is the sum of square [43]. According to the data given in Table 3, a high correlation coefficient (R^2 = 0.953) between the predicted and experimental CR (%) was obtained, which indicated that the applied model can be reliable for predicting CR (%). The plot of predicted CR (%) vs. experimental CR (%) is depicted in Fig. 3(a), exhibiting good agreement between the predicted and experimental CR (%). The correlation coefficient of 0.953 demonstrated that 95.3% of the variations for CR (%) are explained by the model, but the model does not explain 4.7% of the variations of CR (%) [44]. In addition, the value of adjusted R^2 adjusts the value of R^2 regarding the sample size and the number of operational parameters and statistical terms based on the degrees of freedom [29,45]. From the other point of view, adjusted R^2 modifies R^2 by taking into consideration the number of covariates in the model. The value of adjusted R^2 for the adsorption of DB71 onto biosilica/CA nanobiocomposite was calculated through Eq. (5):

$$\text{Adjusted } R^2 = 1 - ((n-1)/(n-p)(1-R^2)) \quad (5)$$

where n and p are the number of experimental runs and predictors in the CCD model, respectively [43]. The obtained value for adjusted R^2 (0.913) was close to the value of R^2 (0.953), suggesting a good fitness between the predicted and experimental CR (%). As can be seen from Table 3, the high value of adequate precision (18.94) and low value obtained for the coefficient of variation (CV = 8.12%) indicated suitability of the applied model for the prediction of CR (%) under different experimental conditions. The preferred value for "adequate precision" is greater than 4 [28]. Residuals, which can be obtained through calculation of the difference between the experimental and predicted CR (%), exhibit how well the applied model satisfies the assumptions of ANOVA [42,45]. The plots of residuals vs. run number, predicted CR (%), and experimental CR (%) were depicted in Fig. 3(b–d), respectively. As illustrated, the residuals towards run number, predicted CR (%), and experimental CR (%) are randomly distributed, implying normal distribution of the residuals. One of the approaches, which can be used for the evaluation of the importance of individual and interactive effects of the operational parameters, is the comparison of F- and p-values obtained for each model term. The larger the quantity of the F-values and smaller p-values, the more meaningful is the corresponding coefficient estimate [42,44]. Among individual effects, the initial DB71 concentration (x_1) with F-value of 179.5 and p-value of 0.0001 produces the largest effect on CR (%), while the initial pH (x_4) with F-value of 16.79 and p-value of 0.0008 produced the lowest individual effect on CR (%). As given in

Table 2
Experimental and predicted results for the adsorption of DB71 onto biosilica/CA nanobiocomposite

	Coded parameters				Actual parameters				Color removal (%)	
Run no.	X_1	X_2	X_3	X_4	X_1	X_2	X_3	X_4	Experimental CR (%)	Predicted CR (%)
1	+1	+1	+2	+1	40	2.0	50	9	52.33	53.12
2	0	0	0	−1	30	1.5	35	3	69.23	65.76
3	+1	+1	−1	−2	40	2.0	20	5	47.23	48.06
4	0	+2	0	0	30	2.5	35	7	73.12	66.04
5	0	0	0	0	30	1.5	35	7	62.08	64.32
6	0	0	0	0	30	1.5	35	7	65.79	64.32
7	+1	−1	+1	+1	40	1.0	50	9	43.21	42.38
8	0	0	0	0	30	1.5	35	7	69.49	64.32
9	0	0	0	+2	30	1.5	35	11	46.04	50.01
10	−1	−1	−1	−1	20	1.0	20	5	60.02	58.34
11	−1	−1	+1	+1	20	1.0	50	9	71.22	69.50
12	+1	+1	+1	−1	40	2.0	50	5	58.11	62.60
13	+1	−1	−1	+1	40	1.0	20	5	31.49	29.34
14	+1	−1	+1	−1	40	1.0	50	5	47.65	48.79
15	−1	+1	+1	−1	20	2.0	50	5	81.32	85.33
16	−1	−1	−1	+1	20	1.0	20	9	56.16	52.06
17	0	−2	0	0	30	0.5	35	7	33.61	41.19
18	0	0	0	0	30	1.5	35	7	63.45	64.32
19	+1	−1	−1	+1	40	1.0	20	9	28.17	23.27
20	0	0	0	0	30	1.5	35	7	66.45	64.32
21	+1	+1	−1	+1	40	2.0	20	9	37.11	38.92
22	+1	+1	−1	+1	20	2.0	20	9	65.13	63.10
23	0	0	0	0	30	1.5	35	7	60.11	64.32
24	+1	0	0	0	50	1.5	35	7	30.74	29.90
25	0	0	−1	0	30	1.5	5	7	36.35	41.60
26	−1	+1	+1	+1	20	2.0	50	9	73.11	75.64
27	−1	−1	+1	−2	20	1.0	50	5	77.54	76.12
28	−1	+1	−1	−1	20	2.0	20	5	71.23	72.45
29	0	0	+2	0	30	1.5	65	7	78.33	73.58
30	0	0	0	0	30	1.5	35	7	62.87	64.32
31	−2	0	0	0	10	1.5	35	7	80.08	81.42

Table 3
The results of ANOVA for the adsorption of DB71 onto biosilica/CA nanobiocomposite

Source	Sum of squares	Degree of freedom	Mean square	*F*-value	*p*-value	
Regression	7,254.10	14	518.15	23.36	0.0001	Significant
Residuals	354.85	16	22.18			
Lack of fit	295.85	10	29.59	3.01	0.0953	Not significant
Pure error	59.03	6	9.84			
Total	7,608.98	30				

Notes: R^2 = 0.953, adjusted R^2 = 0.913, adequate precision = 18.94, coefficient of variation (CV) = 8.12 (%).

Table 4, the interactive effects (x_{12} with *F*-value of 0.96, x_{13} with *F*-value of 0.12, x_{14} with *F*-value of 0.002, x_{23} with *F*-value of 1.08, x_{24} with *F*-value of 0.42 and x_{34} with *F*-value of 0.005) produced lower effects on CR (%) in comparison with individual effects. Obviously, the interactive effect of adsorbent dosage and contact time (x_{23}) caused the greatest interactive effects, while the interactive effect of initial DB71 concentration and initial pH (x_{14}) caused the lowest interactive effects.

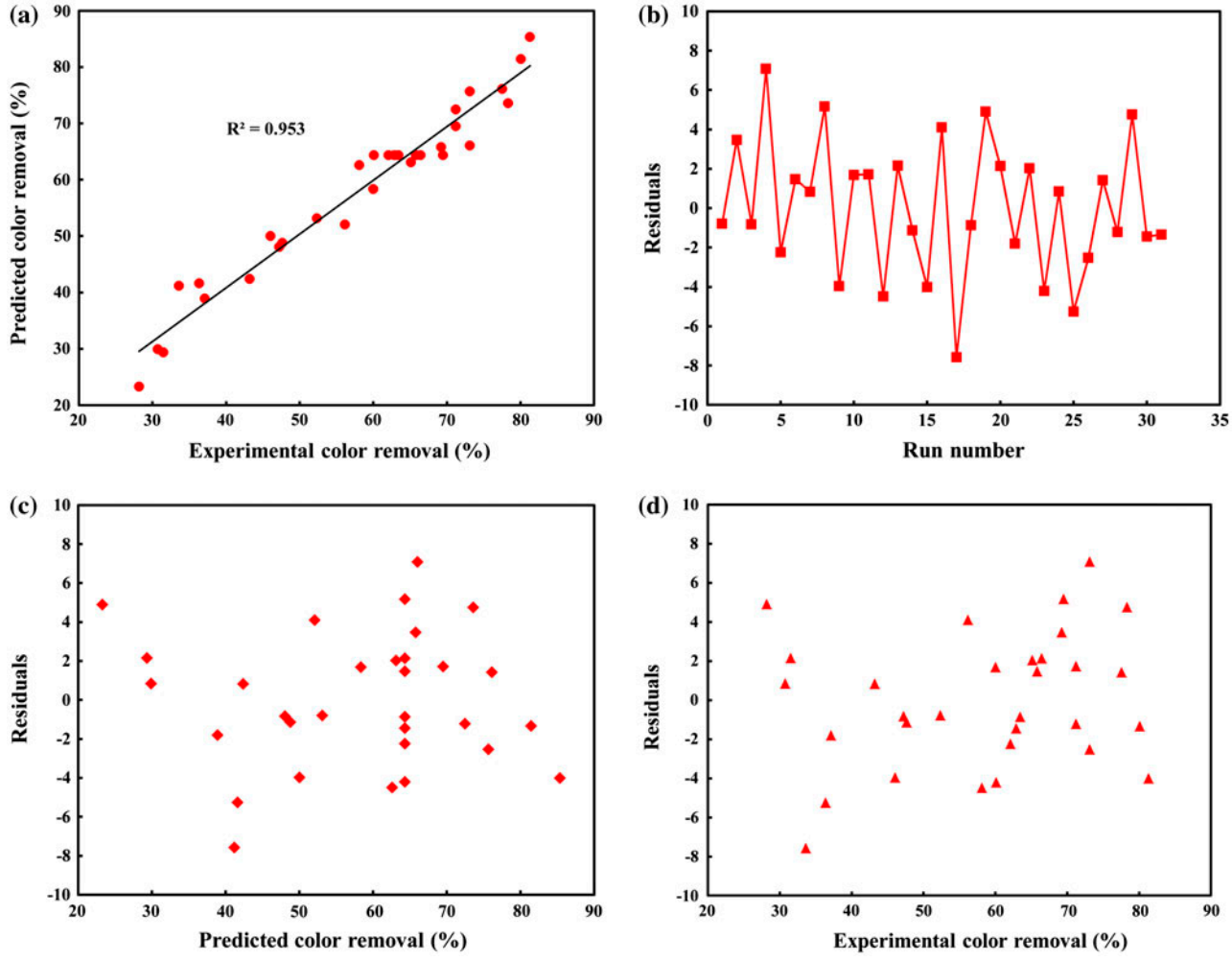

Fig. 3. Predicted color removal vs. experimental color removal (a) and together with corresponding residual plots ((b)–(d)).

3.3. The effect of operational parameters

Response surface plots and corresponding contour plots were employed to study the interactive effects of various operational parameters on the adsorption of DB71 from aqueous phase. The response surface plots (3-D) of the response as a function of two independent parameters can be beneficial in understanding the interactive effects of selected independent parameters [29]. Fig. 4(a) and (b) shows the effect of initial DB71 concentration on CR (%), where the adsorbent dosage and initial pH were constant at 1.5 g/L and 7, respectively. As shown, increasing initial DB71 concentration from 10 to 50 mg/L resulted in decreasing CR (%) within contact time of 65 min. At lower initial dye concentrations, all dye molecules will be adsorbed onto adsorptive sites, resulting in higher CR (%). The lower CR (%) at higher dye concentrations can be due to the saturation of adsorptive sites of the nanobiocomposite [19]. Similar result has been reported by Chen and Lin in the adsorption of Reactive red 22 by immobilized biomass in alginate–silicate sol–gel beads [3]. Fig. 5(a) and (b) exhibited that how increasing adsorbent dosage and contact time led to increasing CR (%), where the initial DB71 concentration and initial pH were constant at 30 mg/L and 7, respectively. Increasing CR (%) with adsorbent dosage can be ascribed to the increased adsorbent surface and adsorptive sites for sequestering dye molecules in aqueous phase [23,46]. As shown in Fig. 6(a) and (b), the CR (%) was gradually increased with decreasing initial pH along with increasing contact time. In this set of experiments, the initial DB71 concentration and adsorbent dosage were constant at 30 mg/L and 1.5 g/L, respectively. Enhanced adsorption of DB71 by the nanobiocomposite at acidic pH values can be attributed to the protonation of the surface of

Table 4
Estimated regression coefficient and corresponding *F*- and *p*-values obtained during CCD for the adsorption of DB71 onto biosilica/CA nanobiocomposite

Coefficient	Coefficient estimate	Standard error	*F*-value	*p*-value
x_0	64.32	1.78	23.36	0.0001
x_1	−12.88	0.96	179.5	0.0001
x_2	6.21	0.96	41.78	0.0001
x_3	8.00	0.96	69.19	0.0001
x_4	−3.94	0.96	16.79	0.0008
x_{12}	1.15	1.18	0.960	0.3440
x_{13}	0.42	1.18	0.120	0.7287
x_{14}	0.052	1.18	0.002	0.9654
x_{23}	−1.23	1.18	1.080	0.3134
x_{24}	−0.77	1.18	0.420	0.5241
x_{34}	−0.084	1.18	0.005	0.9438
x_{11}	−2.16	0.88	6.040	0.0258
x_{22}	−2.68	0.88	9.230	0.0078
x_{33}	−1.68	0.88	3.650	0.0742
x_{44}	−1.61	0.88	3.340	0.0865

adsorbent and subsequently electrostatic attraction between negatively charged anionic dye and positively charged surface of the nanobiocomposite [47], while increasing initial pH resulted in increasing the number of negatively charged sites on the surface of the nanobiocomposite leading to the electrostatic repulsion between anionic dye molecules and negatively charged sites on the surface of the adsorbent [14]. Three-dimensional surface plot (Fig. 6(a)) and corresponding contour plot (Fig. 6(b)) of the effect of initial pH indicated a little increment in the CR (%) with decreasing initial pH.

3.4. Numerical optimization of decolorization process

To reach optimized values of the operational parameters for the maximum CR (%), numerical optimization was applied in which the CR (%) as response was set to "maximize" and the operational parameters were set to "in range." The result of numerical optimization showed that a maximized CR (%) of 81.49% can be achievable with initial DB71 concentration of 21 mg/L, adsorbent dosage of 2.4 g/L, contact time of 42 min, and initial pH of 5. Additionally, confirmatory experiments were performed under optimized values to verify the result of numerical optimization. As result, a mean value of 84.06 ± 3.58% was obtained for CR (%) during the confirmatory experiments under optimum operational parameters, indicating the reliability of applied model for the estimation of real conditions.

3.5. Thermodynamic study

The thermodynamic study was accomplished via changing the solution temperature between 293 and 313 K according to the "0" level of the range of studied operational parameters (DB71 concentration of 30 mg/L, adsorbent dosage of 1.5 g/L and initial pH of 7) within contact time of 60 min. The Gibbs free energy (ΔG°) (kJ/mol), entropy change (ΔS°) (kJ/mol K), and enthalpy change (ΔH°) (kJ/mol) for the adsorption of DB71 onto biosilica/CA nanobiocomposite were estimated via Eqs. (6) and (7):

$$\Delta G^\circ = -RT \ln K_D \tag{6}$$

$$\ln K_D = (\Delta S^\circ/R) - (\Delta H^\circ/RT) \tag{7}$$

where T (K), K_D (q_e/C_e), and R are the temperature of solution, distribution coefficient, and the universal gas constant, respectively [39,48,49]. The value of ΔH° and ΔS° were gained through the slope ($-\Delta H/R$) and intercept ($\Delta S/R$) of the plot of $\ln K_D$ vs. $1/T$. The values of thermodynamic parameters are listed in Table 5. As shown, the obtained negative values for ΔG° and ΔH° demonstrated spontaneous and exothermic nature of the adsorption of DB71 onto the nanobiocomposite. The high value of ΔH° showed a moderately strong binding between the adsorbed DB71 and the surficial functional groups of the nanobiocomposite. Besides, the negative value of ΔS° implies lower degree of freedom of adsorbed DB71 and subsequently strong

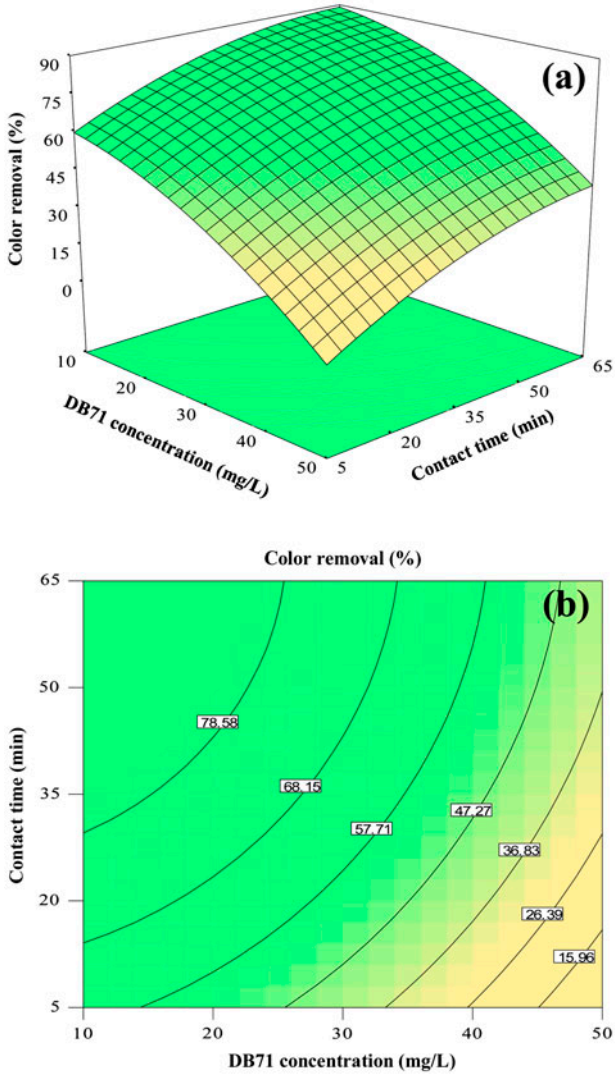

Fig. 4. Three-dimensional plot (a) and corresponding contour plot (b) for interactive effect of initial dye concentration and reaction time.

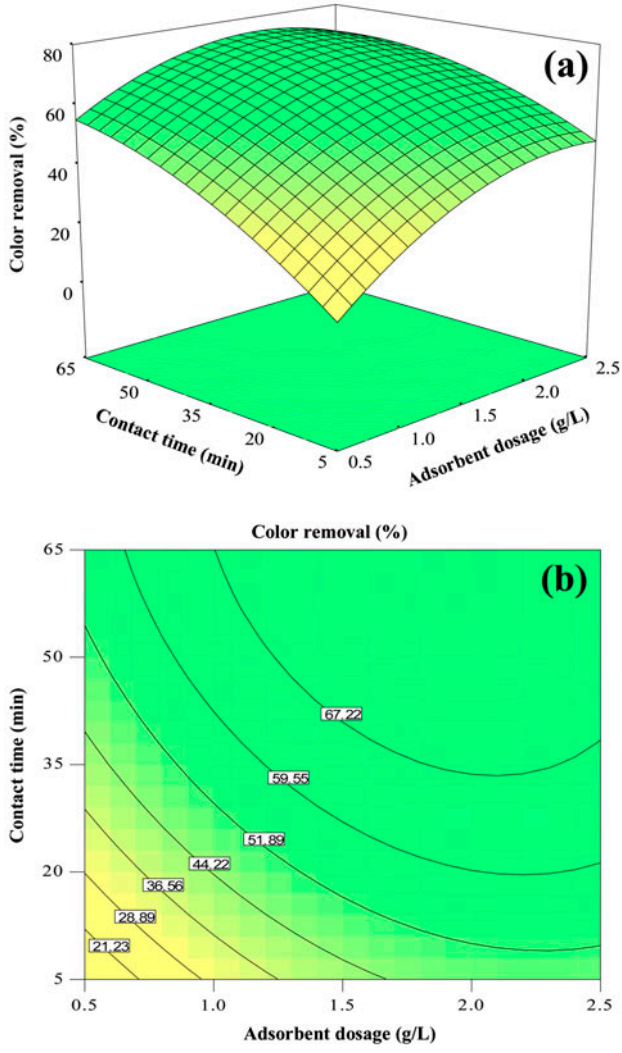

Fig. 5. Three-dimensional plot (a) and corresponding contour plot (b) for interactive effect of adsorbent dosage and reaction time.

attraction between the adsorbate molecules and surficial functional groups of the nanobiocomposite [50].

3.6. Kinetic study

Predicting the rate of adsorption process is one of the most important factors during designing adsorption systems to be used in full-scale applications [46]. The pseudo-first- and pseudo-second-order kinetic models were employed to reach a better understanding of the mechanism of DB71 removal through the adsorption onto biosilica/CA nanobiocomposite. The kinetic study was carried out at an initial DB71 concentration of 30 mg/L, adsorbent dosage of 1.5 g/L, and initial pH of 7 within contact time of 60 min. The adsorption of DB71 onto biosilica/CA nanobiocomposite reached equilibrium within 60 min and further increase in contact time did not significantly increase the amount of adsorbed dye (data not shown). The linear form of the pseudo-first-order kinetic model is shown through Eq. (8):

$$\log(q_e - q_t) = \log q_e - (k_{1,ads}/2.303)t \quad (8)$$

where q_t and $k_{1,ads}$ are the amount of adsorbed DB71 at time t (mg/g) and the rate constant (1/min), respectively [51]. To depict the linear regression of the pseudo-first-order model, $\log(q_e - q_t)$ was plotted vs. t. Based on the equation of linear regression, kinetic

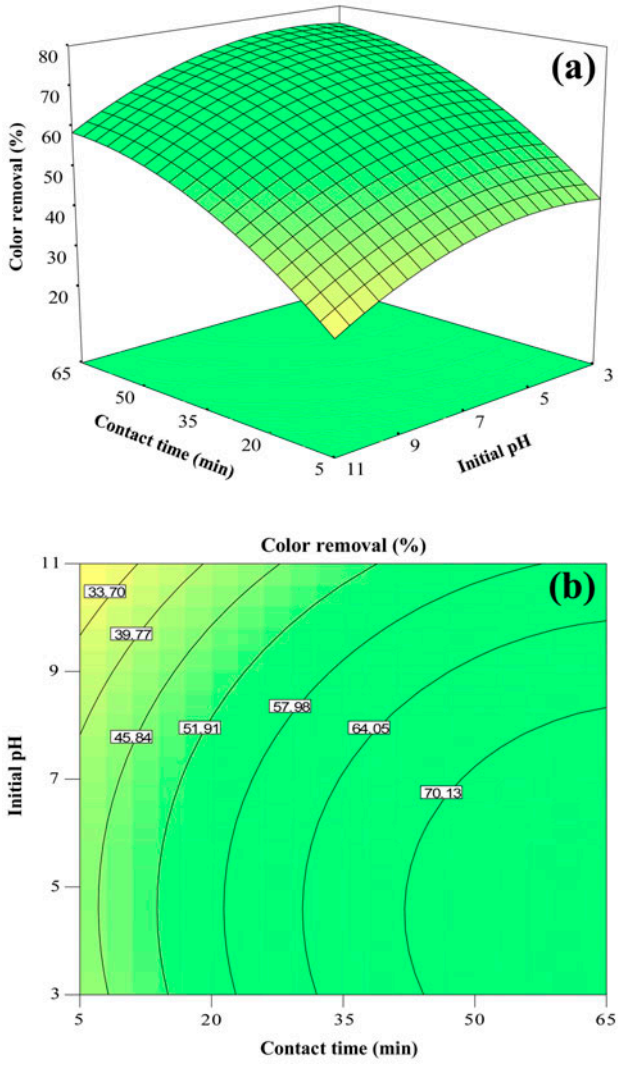

Fig. 6. Three-dimensional plot (a) and corresponding contour plot (b) for interactive effect of initial pH and reaction time.

parameters corresponding to the pseudo-first-order model were determined. The intercept and slope of the plot determine the values of q_e and $k_{1,ad}$, respectively. In addition, the linear form of the pseudo-second-order kinetic model is displayed in Eq. (9):

$$t/q_t = (1/k_{2,ad}q_e^2) + (1/q_e)t \quad (9)$$

where $k_{2,ads}$ is the rate constant of second-order equation (g/mg min) [23,52,53]. The values of q_e and $k_{2,ad}$ can be calculated from the slope and intercept of the plot of t/q_t vs. t, respectively. The results of kinetic study are provided in Table 6. According to the higher correlation coefficient of the pseudo-second-order model (R^2 = 0.977) in comparison with the pseudo-first-order model (R^2 = 0.949), it can be stated that the adsorption of DB71 onto biosilica/CA nanobiocomposite follows pseudo-second-order kinetic model. This demonstrated that several mechanisms are involved in the adsorption of DB71. Additionally, fitness of the adsorption process to the pseudo-second-order kinetic model indicated that chemical adsorption is the sole rate-limiting step for the adsorption of DB71 onto biosilica/CA nanobiocomposite [6,8,51]. Generally, it has been exhibited that the kinetic adsorption is generally better described by the pseudo-second-order kinetic model for the adsorption of both cationic and anionic dyes in aqueous solutions [51,54].

3.7. Isotherm study

To carry out the isotherm study, initial DB71 concentration was varied between 10 and 50 mg/L, while adsorbent dosage, contact time, and initial pH were constant at 1.5 g/L, 60 min, and 7, respectively. The linearized forms of Langmuir, Freundlich, and Dubinin–Radushkevich (D–R) isotherm models were used to describe the adsorption of DB71 onto biosilica/CA nanobiocomposite. The linearized form of Langmuir isotherm model is exhibited in Eq. (10):

$$C_e/q_e = 1/Kq_m + C_e/q_m \quad (10)$$

where q_m (mg/g) and K (L/mg) are the maximum amount of adsorbed dye molecules and the affinity of the binding sites for sequestering the adsorbate (Langmuir constant), respectively [14,34]. The values of q_m and K can be calculated from the slope and

Table 5
The results of thermodynamic study for the adsorption of DB71 onto biosilica/CA nanobiocomposite

Temperature (K)	(ΔG°) (kJ/mol)	(ΔS°) (kJ/mol K)	(ΔH°) (kJ/mol)
298	−0.474	−0.023	−7.311
303	−0.340		
308	−0.263		
313	−0.118		
318	−0.011		

Table 6
The results of kinetic study for the adsorption of DB71 onto biosilica/CA nanobiocomposite

Type of kinetic model	Value
Pseudo-first-order model	
R^2	0.949
$k_{1,ads}$ (1/min)	0.044
q_e (mg/g)	14.29
Pseudo-second-order model	
R^2	0.977
$k_{2,ads}$ (g/mg min)	0.004
q_e (mg/g)	18.59
$q_{experimental}$ (mg/g)	16.81

intercept of the plot of C_e/q_e vs. C_e, respectively. The linearized form of Freundlich isotherm model is shown through Eq. (11):

$$\log q_e = \log K_F + 1/n \log C_e \quad (11)$$

where q_e (mg/g) is the amount of adsorbed dye and C_e (mg/L) is the residual dye concentration in solution. The sorption capacity and sorption intensity can be determined via K_F (L/g) and n as Freundlich constants, respectively [5,46]. The values of K_F and n were calculated from intercept and slope of the plot of log q_e vs. log C_e, respectively. The application of D–R isotherm model can be useful to determine whether the adsorption process is chemical or not. The linear form of D–R isotherm model and corresponding parameters were characterized via Eqs. (12) and (13):

$$\ln Q = \ln Q_m - k\varepsilon^2 \quad (12)$$

$$\varepsilon = RT \ln(1 + 1/C_e) \quad (13)$$

where Q, Q_0, k, ε, R, *and* T are the amount of adsorbed dye (mol/g), adsorption capacity (mol/g), adsorption energy (mol^2/J^2), Polanyi potential (J^2/mol^2), universal gas constant (8.314 J/mol K), and temperature (K), respectively [23,34]. The values of Q_0 and k were obtained from intercept and slope of the plot of log Q vs. ε^2, respectively. The results of isotherm study are provided in Table 7. As result, the Langmuir isotherm model was the best isotherm model for describing the adsorption of DB71 onto the nanobiocomposite (R^2 = 0.994) with a maximum adsorption capacity of 21.32 mg/g. In accordance with our results, Salehi and coworkers found that the adsorption of Direct Blue 78 onto chitosan–zinc oxide nanoparticle was well fitted to Langmuir isotherm model [14]. The separation factor (R_L) associated with the Langmuir isotherm

Table 7
Isotherm parameters for the adsorption of DB71 onto biosilica/CA nanobiocomposite

Type of isotherm models	Values
Langmuir isotherm	
q_{max} (mg/g)	21.32
K (L/mg)	0.0193
R_L	0.510–0.838
R^2	0.9940
Freundlich isotherm	
K_F (L/g)	5.379
n	2.611
R^2	0.8980
Dubinin–Radushkevich (D–R) isotherm	
k (mol^2/J^2)	3×10^{-9}
Q^0 (mol/g)	0.0001
E (kJ/mol)	12.91
R^2	0.9142

model was used to specify the suitability of the adsorption process as expressed via Eq. (14):

$$R_L = 1/(1 + C_0 K) \quad (14)$$

where C_0 is the initial adsorbate concentration (mg/L) and K is the Langmuir constant (L/mg). If the values of R_L are between 0 and 1, the adsorption process would be favorable [39,52,55]. Thus, the obtained values for R_L, which were between 0.510 and 0.838, indicated that the adsorption of DB71 onto biosilica/CA nanobiocomposite would be favorable. In the following, the mean free energy of adsorption (E) was calculated and used to determine the nature of the process as shown in Eq. (15):

$$E = 1/(-2k)^{0.5} \quad (15)$$

If the value of E is between 8 and 16 kJ/mol, the adsorption process is chemical. Alternatively, if the value of E is less than 8 kJ/mol, the process would be physical [23,34]. The value of E for the adsorption of DB71 onto biosilica/CA nanobiocomposite was obtained to be 12.91 kJ/mol, confirming chemical nature of the adsorption process.

4. Conclusions

In the present work, nano-sized biosilica was entrapped by CA and used for removing a textile dye in aqueous solutions. CCD statistical approach was

employed to vigorously evaluate the effect of operational parameters on the decolorization and to determine the optimum values of operational parameters for the highest color removal. For a color removal of 81.49%, the initial dye concentration, adsorbent dosage, contact time, and initial pH were identified to be 21 mg/L, 2.4 g/L, 42 min, and 7, respectively. Thermodynamic parameters indicated spontaneous and exothermic nature of the adsorption process. The results of isotherm study showed that the adsorption of DB71 obeyed Langmuir model with the maximum adsorption capacity of 21.32 mg/g. In addition, the mean free energy of adsorption (E) revealed the chemical nature of the adsorption process. Conclusively, the application of nano-sized biosilica in immobilized form could be an efficient approach for treating colored effluents.

Acknowledgments

The authors would like to thank Arak University of Medical Sciences (Iran) and University of Tabriz (Iran) for their financial and instrumental supports.

References

[1] Z. Noorimotlagh, R. Darvishi Cheshmeh Soltani, A.R. Khataee, S. Shahriyar, H. Nourmoradi, Adsorption of a textile dye in aqueous phase using mesoporous activated carbon prepared from Iranian milk vetch, J. Taiwan Inst. Chem. Eng. 45 (2014) 1783–1791.

[2] Y. Kalpaklı, Ş. Toygun, G. Köneçoğlu, M. Akgün, Equilibrium and kinetic study on the adsorption of basic dye (BY28) onto raw Ca-bentonite, Desalin. Water Treat. (2013), doi: 10.1080/19443994.2013.830804 (in press).

[3] J.-P. Chen, Y.-S. Lin, Decolorization of azo dye by immobilized *Pseudomonas luteola* entrapped in alginate–silicate sol–gel beads, Process Biochem. 42 (2007) 934–942.

[4] R.Darvishi Cheshmeh Soltani, A.R. Khataee, M. Safari, S.W. Joo, Preparation of bio-silica/chitosan nanocomposite for adsorption of a textile dye in aqueous solutions, Int. Biodeterior. Biodegrad. 85 (2013) 383–391.

[5] R. Darvishi Cheshmeh Soltani, A. Rezaee, G. Shams Khorramabadi, K. Yaghmaeian, Optimization of lead (II) biosorption in an aqueous solution using chemically modified aerobic digested sludge, Water Sci. Technol. 63 (2011) 129–135.

[6] R. Darvishi Cheshmeh Soltani, G.H. Shams Khorramabadi, A.R. Khataee, S. Jorfi, Silica nanopowders/alginate composite for adsorption of lead (II) ions in aqueous solutions, J. Taiwan Inst. Chem. Eng. 45 (2013) 973–980.

[7] M. Matto, Q. Husain, Decolorization of textile effluent by bitter gourd peroxidase immobilized on concanavalin a layered calcium alginate–starch beads, J. Hazard. Mater. 164 (2009) 1540–1546.

[8] G.S. Khorramabadi, R.D.C. Soltani, A. Rezaee, A.R. Khataee, A. Jonidi Jafari, Utilisation of immobilised activated sludge for the biosorption of chromium (VI), Can. J. Chem. Eng. 90 (2012) 1539–1546.

[9] A. Nejib, D. Joelle, A. Fadhila, G. Sophie, T.-A. Malika, Adsorption of anionic dye on natural and organophilic clays: Effect of textile dyeing additives, Desalin. Water Treat. (2014), doi: 10.1080/19443994.2014.895781 (in press).

[10] A. Mittal, Adsorption kinetics of removal of a toxic dye, Malachite Green, from wastewater by using hen feathers, J. Hazard. Mater. 133 (2006) 196–202.

[11] S. Karaca, A. Gürses, Ö. Açışlı, A. Hassani, M. Kıranşan, K. Yıkılmaz, Modeling of adsorption isotherms and kinetics of Remazol Red RB adsorption from aqueous solution by modified clay, Desalin. Water Treat. 51 (2013) 2726–2739.

[12] S. Noreen, H.N. Bhatti, S. Nausheen, S. Sadaf, M. Ashfaq, Batch and fixed bed adsorption study for the removal of Drimarine Black CL-B dye from aqueous solution using a lignocellulosic waste: A cost affective adsorbent, Ind. Crops Prod. 50 (2013) 568–579.

[13] G. Sharma, M. Naushad, D. Pathania, A. Mittal, G.E. El-desoky, Modification of *Hibiscus cannabinus* fiber by graft copolymerization: Application for dye removal, Desalin. Water Treat. (2014), doi: 10.1080/19443994.2014.904822 (in press).

[14] R. Salehi, M. Arami, N.M. Mahmoodi, H. Bahrami, S. Khorramfar, Novel biocompatible composite (Chitosan–zinc oxide nanoparticle): Preparation, characterization and dye adsorption properties, Colloids Surf., B 80 (2010) 86–93.

[15] R. Rostamian, M. Najafi, A.A. Rafati, Synthesis and characterization of thiol-functionalized silica nano hollow sphere as a novel adsorbent for removal of poisonous heavy metal ions from water: Kinetics, isotherms and error analysis, Chem. Eng. J. 171 (2011) 1004–1011.

[16] M. Zarezadeh-Mehrizi, A. Badiei, A.R. Mehrabadi, Ionic liquid functionalized nanoporous silica for removal of anionic dye, J. Mol. Liq. 180 (2013) 95–100.

[17] R. Darvishi Cheshmeh Soltani, M. Safari, A. Rezaee, H. Godini, Application of a compound containing silica for removing ammonium in aqueous media, Environ. Prog. Sustain. Energy (2014), doi: 10.1002/ep.11969 (in press).

[18] A.R. Cestari, E.F.S. Vieira, A.M.G. Tavares, R.E. Bruns, The removal of the indigo carmine dye from aqueous solutions using cross-linked chitosan—Evaluation of adsorption thermodynamics using a full factorial design, J. Hazard. Mater. 153 (2008) 566–574.

[19] R. Aravindhan, N.N. Fathima, J.R. Rao, B.U. Nair, Equilibrium and thermodynamic studies on the removal of basic black dye using calcium alginate beads, Colloids Surf., A 299 (2007) 232–238.

[20] B.-E. Wang, Y.-Y. Hu, Comparison of four supports for adsorption of reactive dyes by immobilized *Aspergillus fumigatus* beads, J. Environ. Sci. 19 (2007) 451–457.

[21] F. An, B. Gao, Adsorption of phenol on a novel adsorption material PEI/SiO_2, J. Hazard. Mater. 152 (2008) 1186–1191.

[22] M.-Y. Chang, R.-S. Juang, Equilibrium and kinetic studies on the adsorption of surfactant, organic acids and dyes from water onto natural biopolymers, Colloids Surf., A 269 (2005) 35–46.

[23] S.K. Nadavala, K. Swayampakula, V.M. Boddu, K. Abburi, Biosorption of phenol and o-chlorophenol from aqueous solutions on to chitosan–calcium alginate blended beads, J. Hazard. Mater. 162 (2009) 482–489.
[24] J.-S. Bae, H.S. Freeman, Aquatic toxicity evaluation of new direct dyes to the *Daphnia magna*, Dyes Pigm. 73 (2007) 81–85.
[25] Y. Li, J.-Q. Shi, R.-J. Qu, M.-B. Feng, F. Liu, M. Wang, Z.-Y. Wang, Toxicity assessment on three direct dyes (D-BLL, D-GLN, D-3RNL) using oxidative stress bioassay and quantum parameter calculation, Ecotoxicol. Environ. Saf. 86 (2012) 132–140.
[26] R. Darvishi Cheshmeh Soltani, A. Rezaee, A. Khataee, Combination of carbon black–ZnO/UV process with an electrochemical process equipped with a carbon black–PTFE-coated gas-diffusion cathode for removal of a textile dye, Ind. Eng. Chem. Res. 52 (2013) 14133–14142.
[27] R. Darvishi Cheshmeh Soltani, A. Rezaee, A.R. Khataee, H. Godini, Optimisation of the operational parameters during a biological nitrification process using response surface methodology, Can. J. Chem. Eng. 92 (2013) 13–22.
[28] R. Darvishi Cheshmeh Soltani, A. Rezaee, H. Godini, A.R. Khataee, A. Hasanbeiki, Photoelectrochemical treatment of ammonium using seawater as a natural supporting electrolyte, Chem. Ecol. 29 (2013) 72–85.
[29] K.P. Singh, S. Gupta, A.K. Singh, S. Sinha, Optimizing adsorption of crystal violet dye from water by magnetic nanocomposite using response surface modeling approach, J. Hazard. Mater. 186 (2011) 1462–1473.
[30] M.D. Pavlović, A.V. Buntić, K.R. Mihajlovski, S.S. Šiler-Marinković, D.G. Antonović, Ž. Radovanović, S.I. Dimitrijević-Branković, Rapid cationic dye adsorption on polyphenol-extracted coffee grounds—A response surface methodology approach, J. Taiwan Inst. Chem. Eng. 45 (2014) 1691–1699.
[31] M. Arulkumar, P. Sathishkumar, T. Palvannan, Optimization of Orange G dye adsorption by activated carbon of *Thespesia populnea* pods using response surface methodology, J. Hazard. Mater. 186 (2011) 827–834.
[32] A.L. Cazetta, O.P. Junior, A.M.M. Vargas, A.P. da Silva, X. Zou, T. Asefa, V.C. Almeida, Thermal regeneration study of high surface area activated carbon obtained from coconut shell: Characterization and application of response surface methodology, J. Anal. Appl. Pyrolysis 101 (2013) 53–60.
[33] A.M.M. Vargas, A.C. Martins, V.C. Almeida, Ternary adsorption of acid dyes onto activated carbon from flamboyant pods (*Delonix regia*): Analysis by derivative spectrophotometry and response surface methodology, Chem. Eng. J. 195–196 (2012) 173–179.
[34] A. Ergene, K. Ada, S. Tan, H. Katırcıoğlu, Removal of Remazol Brilliant Blue R dye from aqueous solutions by adsorption onto immobilized *Scenedesmus quadricauda*: Equilibrium and kinetic modeling studies, Desalination 249 (2009) 1308–1314.
[35] L. Wang, A. Wang, Adsorption properties of Congo Red from aqueous solution onto surfactant-modified montmorillonite, J. Hazard. Mater. 160 (2008) 173–180.
[36] K.-W. Park, J.H. Jung, Spectroscopic and electrochemical characteristics of a carboxylated graphene–ZnO composites, J. Power Sources 199 (2012) 379–385.
[37] M.-C. Wu, J.J.P. Coca, G.R.-L. Chang, S.-Y. Suen, C.-F. Lin, H.-N. Chou, S.-Y. Lai, M.-Y. Wang, Chemical modification of *Nitzschia panduriformis*'s frustules for protein and viral nanoparticle adsorption, Process Biochem. 47 (2012) 2204–2210.
[38] A. Heidari, H. Younesi, Z. Mehraban, Removal of Ni (II), Cd(II), and Pb(II) from a ternary aqueous solution by amino functionalized mesoporous and nano mesoporous silica, Chem. Eng. J. 153 (2009) 70–79.
[39] C.-H. Zhou, D. Zhang, D.-S. Tong, L.-M. Wu, W.-H. Yu, S. Ismadji, Paper-like composites of cellulose acetate–organo-montmorillonite for removal of hazardous anionic dye in water, Chem. Eng. J. 209 (2012) 223–234.
[40] R. Darvishi Cheshmeh Soltani, A. Rezaee, A.R. Khataee, M. Safari, Photocatalytic process by immobilized carbon black/ZnO nanocomposite for dye removal from aqueous medium: Optimization by response surface methodology, J. Ind. Eng. Chem. 20 (2014) 1861–1868.
[41] A.R. Khataee, M. Zarei, S.K. Asl, Photocatalytic treatment of a dye solution using immobilized TiO_2 nanoparticles combined with photoelectro-Fenton process: Optimization of operational parameters, J. Electroanal. Chem. 648 (2010) 143–150.
[42] A.R. Khataee, M. Zarei, L. Moradkhannejhad, Application of response surface methodology for optimization of azo dye removal by oxalate catalyzed photoelectro-Fenton process using carbon nanotube–PTFE cathode, Desalination 258 (2010) 112–119.
[43] A. Haber, R. Runyun, General Statistics. Addison-Wesley, Boston, MA, 1977.
[44] A.R. Khataee, M. Zarei, M. Fathinia, M.K. Jafari, Photocatalytic degradation of an anthraquinone dye on immobilized TiO_2 nanoparticles in a rectangular reactor: Destruction pathway and response surface approach, Desalination 268 (2011) 126–133.
[45] M. Fathinia, A.R. Khataee, M. Zarei, S. Aber, Comparative photocatalytic degradation of two dyes on immobilized TiO_2 nanoparticles: Effect of dye molecular structure and response surface approach, J. Mol. Catal. A: Chem. 333 (2010) 73–84.
[46] N.M. Mahmoodi, Magnetic ferrite nanoparticle–alginate composite: Synthesis, characterization and binary system dye removal, J. Taiwan Inst. Chem. Eng. 44 (2013) 322–330.
[47] M.Ş. Tanyildizi, Modeling of adsorption isotherms and kinetics of reactive dye from aqueous solution by peanut hull, Chem. Eng. J. 168 (2011) 1234–1240.
[48] H. Daraei, A. Mittal, M. Noorisepehr, J. Mittal, Separation of chromium from water samples using eggshell powder as a low-cost sorbent: Kinetic and thermodynamic studies, Desalin. Water Treat. (2013), doi: 10.1080/19443994.2013.837011 (in press).
[49] H. Daraei, A. Mittal, M. Noorisepehr, F. Daraei, Kinetic and equilibrium studies of adsorptive removal of phenol onto eggshell waste, Environ. Sci. Pollut. Res. 20 (2013) 4603–4611.
[50] A. Rahmani, H. Zavvar Mousavi, M. Fazli, Effect of nanostructure alumina on adsorption of heavy metals, Desalination 253 (2010) 94–100.
[51] M.A.M. Salleh, D.K. Mahmoud, W.A.W.A. Karim, A. Idris, Cationic and anionic dye adsorption by agricultural solid wastes: A comprehensive review, Desalination 280 (2011) 1–13.

[52] A. Saeed, M. Iqbal, S.I. Zafar, Immobilization of *Trichoderma viride* for enhanced methylene blue biosorption: Batch and column studies, J. Hazard. Mater. 168 (2009) 406–415.
[53] J. Mittal, D. Jhare, H. Vardhan, A. Mittal, Utilization of bottom ash as a low-cost sorbent for the removal and recovery of a toxic halogen containing dye eosin yellow, Desalin. Water Treat. 52 (2014) 4508–4519.
[54] A. Mittal, V. Thakur, J. Mittal, H. Vardhan, Process development for the removal of hazardous anionic azo dye Congo red from wastewater by using hen feather as potential adsorbent, Desalin. Water Treat. 52 (2013) 227–237.
[55] A. Mittal, Use of hen feathers as potential adsorbent for the removal of a hazardous dye, Brilliant Blue FCF, from wastewater, J. Hazard. Mater. 128 (2006) 233–239.